A Mechanism for Offshore Transport across the Gulf Stream

GUOQING LIN* AND JOSEPH F. ATKINSON

Department of Civil, Structural and Environmental Engineering, State University of New York at Buffalo, Buffalo, New York

29 June 1998 and 23 July 1999

ABSTRACT

This paper explores a possible mechanism to explain an atypical phenomenon observed in the Gulf Stream between the Florida Straits and Cape Hatteras, namely, upgradient momentum transport and associated eddy-to-mean energy conversion on the cyclonic shear side. The proposed mechanism is based on the results of an experimental study of free surface turbulent jets in a rotating system and on theoretical descriptions of rotating shear flows. Unlike field situations, where Coriolis effects are always present, the laboratory experiment provides a convenient means of comparing turbulence characteristics in rotating and nonrotating systems. Rotation is shown to alter turbulence eddy orientation, thus affecting the momentum transport and energy conversion processes.

1. Introduction

The Gulf Stream is a western boundary current separating the northwest coastal ocean from the Sargasso Sea. It has certain jetlike properties with respect to the relative importance of momentum and buoyancy, especially for the reach of the Florida Current between the Florida Straits and Cape Hatteras (Stommel 1965). The main feature of interest for the present paper is the turbulent transport of momentum and associated barotropic energy conversion across the jet stream. For a nonrotating plane jet, mean velocity shear serves as a source for turbulence, and momentum is always transported downgradient, outward from the jet center. Thus, the associated kinetic energy is converted from mean motion to turbulence. This is not the case, however, for the Florida Current, where upgradient momentum transport and the associated eddy-to-mean energy conversion occur on the coastal cyclonic shear side. The phenomenon was first reported by Webster (1961a) in the surface layer of Gulf Stream sections near Miami (about 26°N) and off Onslow Bay, North Carolina (about 35°N). On the Sargasso Sea side of the stream, the shear is anticyclonic and the momentum transport is downgradient of the mean velocity shear, similar to those observed for nonrotating conditions. The momentum and associated energy are thus transported unidirectionally across the Gulf Stream offshore.

The above unusual offshore transports of momentum and energy also were reported for four sections at Miami, Jacksonville, Onslow Bay, and Cape Hatteras (Webster 1965). Schmitz and Niiler (1969) reexamined Webster's estimates, analyzed additional measurements, and confirmed Webster's conclusion about significant eddy-to-mean energy flux in the cyclonic shear side of the Gulf Stream. Brooks and Niiler (1977) later conducted a comprehensive investigation of the energetics of the Florida Current for the whole cross section in the vicinity of Miami. The same phenomenon, upgradient momentum transport and associated eddy-to-mean energy conversion, occurred on the cyclonic shear (Florida coastal) side, not only in the surface layer as reported by Webster, but also in the deep water of the current. This was an ''enigma'' then (Brooks and Niiler 1977) and it is still an ''enigma'' today (P. Niiler 1998, personal communication). Why momentum is transferred upgradient and turbulent energy is converted from eddy to mean motion in this system is not yet clear.

A significant step toward a possible explanation was taken by Webster (1961b), who constructed an idealized elongated eddy, based on measurements crossing a section off Onslow Bay, North Carolina, with the major axis of the eddy leaning along the mean shear. Such an eddy transports momentum upgradient and supplies energy to the mean shear. This kind of eddy structure has been observed from satellite images of the Georgia continental shelf (Lee et al. 1981) and is also suggested in recent measurements of eddy structure in the coastal

* Current affiliation: Skidaway Institute of Oceanography, Savannah, Georgia.

Corresponding author address: Dr. Guoqing Lin, Skidaway Institute of Oceanography, 10 Ocean Science Circle, Savannah, GA 31411.
E-mail: glin@skio.peachnet.edu

current along the southern shore of Lake Ontario (Pal et al. 1998). A field study on the Gulf Stream eddies off Onslow Bay in both winter and summer seasons further confirmed the existence of such an eddy structure and its effects on momentum transport and energy conversion (Bane et al. 1981; Brooks and Bane 1983). Dewar and Bane (1985) also studied the energetics of the Gulf Stream region in the vicinity of the so-called Charleston Bump at about 32°N. Even though the Charleston Bump sets out a major perturbation to the Gulf Stream, momentum is still transported upgradient offshore. The major axes of the eddy ellipses constructed from velocity variances also were found to lean with the mean shear.

The effects of eddy orientation on momentum transport and energy conversion observed by physical oceanographers also have been investigated in studies of rotating homogeneous and shear turbulence. In a homogeneous turbulent flow, rotation has been found to cause alteration of the turbulent structure, as manifested by increasing integral length scales (Ibbetson and Tritton 1975; Jacquin et al. 1990) and by reducing turbulent energy production or decreasing rate of energy transfer from large scales to small scales (Bardina et al. 1985; Cambon and Jacquin 1989; Jacquin et al. 1990; Mansour et al. 1992; Cambon et al. 1997). In a plane shear flow, Bradshaw (1969) suggested an analogy between the gradient Richardson number in a stratified flow and the Bradshaw–Richardson number [renamed as such later by Tritton (1992) and Cambon et al. (1994)] in a nonbuoyant rotating flow. Rotation enhances or suppresses internal instability in a shear flow in the horizontal plane, in the same way that buoyancy does in the vertical plane. Studies of channel flows have shown that the Coriolis forces affect both local and global stability (Lezius and Johnston 1971; Johnston et al. 1972; Kristoffersen and Andersson 1993; Godeferd 1995) and that turbulence eddies are elongated in the streamwise direction. In the cyclonic side, transition to turbulence is suppressed and negative turbulence production may occur. These effects are related to the reorientation of the Reynolds stress tensor by the Coriolis effects in rotating shear flow (Bidokhti and Tritton 1992; Tritton 1992). Specifically, the major principal axis of the Reynolds stress tensor aligns closer to or flips over to the other side of the mean flow direction on the cyclonic side in a rotating fluid, relative to the alignment in a nonrotating fluid.

The key to understanding the turbulent transports of momentum and energy is found in the orientation of the major axis of a turbulence eddy, which corresponds to the major principal axis of the Reynolds stress tensor. How this orientation changes determines the direction and the extent of transport processes. Since the effects of the earth's rotation are always present and these are the very effects that bring about the mean flow of the Gulf Stream, the Coriolis effects on turbulence within the Gulf Stream may have been overlooked in past studies. Laboratory experiments provide a convenient way of comparing transport mechanisms between rotating and nonrotating turbulent jets. Energy conversions from barotropic and baroclinic instability observed in the Gulf Stream seem to be independent of each other, and the former is larger than the latter (Brooks and Niiler 1977; Dewar and Bane 1985). The relevance of dominant barotropic mechanisms in horizontal shear suggests that it may be of interest to study a barotropic fluid. The following section describes an experiment on a free-surface turbulent jet in a rotating system, the results of which show the effects of rotation on the orientation and shape of turbulence eddies.

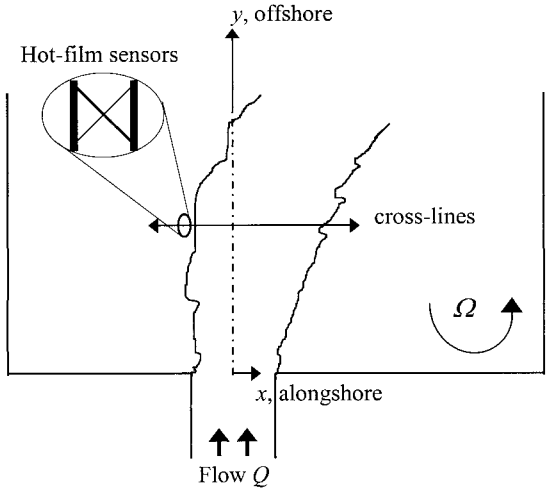

FIG. 1. Schematic of the cross section location for the moving measurements.

2. Rotating surface jet experiment

The experiment was conducted in the Rotating Laboratory Facility at the State University of New York at Buffalo. A test tank 2 m × 3 m in area and 0.3 m deep was installed in a self-contained 3.2 m × 5.3 m rotating room. Water at flow rates up to 1 liter per second was pumped into the tank through an open channel inlet 50 cm long × 15 cm wide and about 1.5 cm deep. Neutrally buoyant surface jets were introduced over a backward-facing step into a quiescent deep water basin. Point measurement stations were distributed in the jet stream over cross-lines parallel to the head wall. The instrumentation consisted primarily of a two-dimensional (2D) cross hot-film probe deployed at depth 1.5 cm, which corresponded to the position of minimum vertical shear effect beneath the surface (Lin 1998). One of the hot-film sensors was oriented 45° (measuring v_1) and another 135° (v_2) counterclockwise from the head wall in the horizontal plane (see Fig. 1). The probe was mounted on a computerized 3D traverse system and velocity signals were digitized using a 12-bit analog-to-

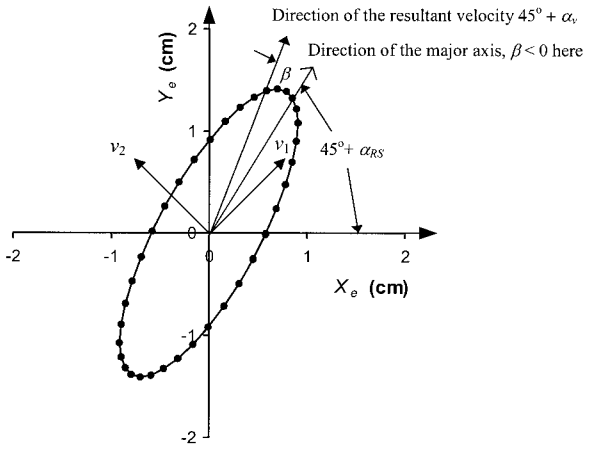

FIG. 2. Illustration of an equivalent turbulent eddy trajectory at a station. The intervals of the points are equal in time. Angle of ν_1 is 45° from the X_e axis, α_ν and α_{RS} are defined relative to ν_1, and β is relative to the direction of the mean resultant velocity.

digital converter. Rotating and nonrotating cases were tested with five different flow rates.

The velocity data were analyzed to form Reynolds stress tensors in the horizontal plane. The principal major and minor axes of the tensor correspond to the maximum and minimum Reynolds normal stresses, respectively. A principal angle, β, was defined as the angle between the orientation of the principal major axis and the corresponding mean resultant velocity direction,

$$\beta = \alpha_{RS} - \alpha_V = \frac{1}{2}\tan^{-1}\frac{2\overline{v_1' v_2'}}{\overline{v_1'^2} - \overline{v_2'^2}} - \tan^{-1}\frac{\overline{v_2}}{\overline{v_1}}, \quad (1)$$

where α_{RS} and α_V are the angles of the principal major axis and the mean resultant velocity, respectively, measured counterclockwise from the v_1 direction (see Fig. 2).

Applying Taylor's frozen turbulence field hypothesis, an equivalent eddy may be constructed from these principal axes. Its streamline is represented by

$$X_e = \frac{\sqrt{\overline{u_\beta'^2}}}{\omega_e}\sin(\omega_e t)\cos\left(\frac{\pi}{4} + \alpha_{RS}\right) + \frac{\sqrt{\overline{v_\beta'^2}}}{\omega_e}\cos(\omega_e t)\sin\left(\frac{\pi}{4} + \alpha_{RS}\right), \quad (2a)$$

$$Y_e = \frac{\sqrt{\overline{u_\beta'^2}}}{\omega_e}\sin(\omega_e t)\sin\left(\frac{\pi}{4} + \alpha_{RS}\right) - \frac{\sqrt{\overline{v_\beta'^2}}}{\omega_e}\cos(\omega_e t)\cos\left(\frac{\pi}{4} + \alpha_{RS}\right), \quad (2b)$$

where X_e and Y_e are Lagrangian coordinates for the equivalent eddy, $\overline{u_\beta'^2}$ and $\overline{v_\beta'^2}$ are the maximum and minimum Reynolds normal stresses, respectively, and ω_e is the equivalent eddy frequency. The X_e axis is parallel to the headwall, and the positive Y_e axis points in the initial surface jet direction offshore. The phase shift of $\pi/4$ represents the angle of the first velocity component measured by the first hot-film sensor (thicker line drawn in Fig. 1) relative to the headwall. The kinetic energy of such an eddy is the same as the measured turbulent kinetic energy in the Eulerian field. An example equivalent eddy with typical eddy frequency of 5 Hz (the inverse of integral timescale) in the experiment is shown in Fig. 2.

The eddies are ellipses in shape for anisotropic turbulence, which is prevalent in shear flows. In a nonrotating plane jet, the principal angle β is antisymmetrically distributed across the jet stream with respect to the center. The eddies lean against the mean shear on both sides; that is, the orientation of the major axes of the eddies is outward from the jet center (Gutmark and Wygnanski 1976). Such oriented eddies are energized by mean velocity shear and momentum is transported downgradient. With the influence of rotation, however, the orientation of the principal major axis shifts anticyclonically (rightward in the Northern Hemisphere) with respect to the mean flow on both sides of a rotating jet, which turns anticyclonically on its own.

Figure 3 shows the results of the principal angle calculations obtained from the experiment. The horizontal axes represent the nondimensional transverse distance, scaled by the longitudinal distance from the ''virtual origin'' of the jet [defined by fitting jet trajectory data to the theoretical calculations of Savage and Sobey (1975)]. For rotating cases, the transverse distance is measured from local centers of the jet trajectories (for detailed calculations, see Lin 1998). Although the data are scattered, the trends of the principal angle values are identifiable and it is the difference of the trends between rotating and nonrotating jets that is important. Compared with the trend in nonrotating jets, the effect of rotation makes the orientation of the major ellipse axis lean closer to (even flip over to) the mean velocity direction in the cyclonic side.

Accompanying the orientation shift of the turbulence eddy is the shape change by the Coriolis effects. The eddy shape may be parameterized by ellipticity K,

$$K = \frac{\overline{u_\beta'^2} - \overline{v_\beta'^2}}{\overline{u_\beta'^2} + \overline{v_\beta'^2}}. \quad (3)$$

This definition of ellipticity is different from that used in plane geometry, but provides the same indication of the extent of departure from eddy circularity. The present definition is preferable here because it can be related to the physical processes of turbulence generation (by shear) and redistribution (by pressure–strain correlation) (Tennekes and Lumley 1972). With a larger value of K, the elliptic motion is closer to a linear oscillation, the turbulence field is more anisotropic and the Coriolis effects (working against pressure–strain

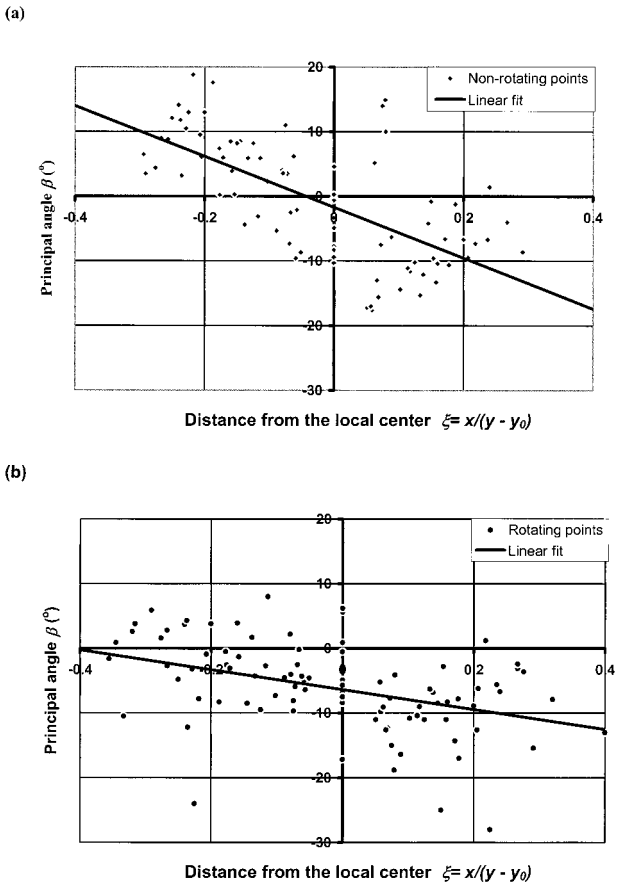

FIG. 3. Scatterplot of the principal angle with distance from local center for (a) nonrotating jets and (b) rotating jets for five different flow rates. The linear fitted lines are intended to show the difference in trends only. The virtual origin y_0 of the jets is estimated from fitting the experimental trajectory to the theoretical path (Lin 1998).

correlation) are more pronounced on turbulent energy redistribution.

Results from the current experiment are shown in Fig. 4. In this figure, results are presented in terms of the entry Froude number and a global Rossby number. The global Rossby number is defined in terms of the average entry velocity and jet penetration length scale L (see Savage and Sobey 1975). This is done for convenience in comparing different tests in the experiment. (It is shown later that a Rossby number based on local velocity shear bears more relevance to the present study.) For the nonrotating cases (open symbols in Fig. 4), the ellipticity K remains at about 0.4 along the jet center, which is the value suggested by Tennekes and Lumley (1972) for a plane jet. In addition, this value compares favorably with a well-designed plane jet [calculated from the experimental data of Gutmark and Wygnanski (1976); see Lin (1998) for details]. For the rotating cases (solid symbols in Fig. 4), the jet undergoes geostrophic adjustment. The ellipticity K starts from about 0.4 close to the mouth of the discharge, as though the jet were not subject to the background rotation, and then increases to a value of about 0.8. The effect of rotation on eddy ellipticity gradually strengthens as the jet adjusts itself to geostrophic flow.

3. Discussion

The experimental results show the effects of rotation on the turbulence structure through eddy orientation and shape changes. The present analysis is focused on two-dimensional turbulence, although it is recognized that, in general, vertical motions may affect the Coriolis effects on the horizontal turbulence structure. However, since the two-dimensional velocities were measured at the depth of minimum vertical shear, it is expected that this effect should be a relatively minor quantitative adjustment, without changing the general conclusions described here. Discussion of the Coriolis effects on shear stability is presented first, followed by descriptions of

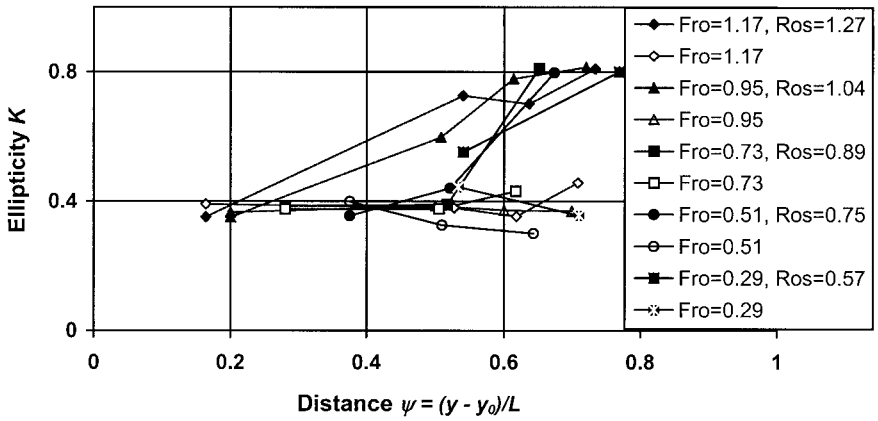

FIG. 4. Comparison of turbulence ellipticity development along the jet stream center line. In the legend, Ro_s is the global Rossby number and Fr_0 is the entrance Froude number. Nonrotating cases are those without Ro_s values in the legend box (open symbols).

turbulent kinetic energy redistribution and a qualitative relationship between rotation intensity and the turbulence structure parameters.

For a homogeneous inviscid fluid with background rotation in the vertical direction, the linearized equations of the fluctuating momentum components in a two-dimensional flow may be written as

$$\frac{\partial u'}{\partial t} + U\frac{\partial u'}{\partial x} + v'\frac{\partial U}{\partial y} - 2\Omega v' = -\frac{1}{\rho}\frac{\partial p'}{\partial x} \quad (4a)$$

and

$$\frac{\partial v'}{\partial t} + U\frac{\partial v'}{\partial x} + 2\Omega u' = -\frac{1}{\rho}\frac{\partial p'}{\partial y}, \quad (4b)$$

where U is mean velocity in the x direction, u' and v' are velocity fluctuations in the x and y directions respectively, p' is pressure fluctuation, Ω is angular speed of the system, ρ is fluid density, and t is time. Eliminating component u' from the above two equations results in

$$\left(\frac{\partial}{\partial t} + U\frac{\partial}{\partial x}\right)^2 v' + 2\Omega\left(2\Omega - \frac{\partial U}{\partial y}\right)v' = \frac{2\Omega}{\rho}\frac{\partial p'}{\partial x} - \frac{1}{\rho}\left(\frac{\partial}{\partial t} + U\frac{\partial}{\partial x}\right)\frac{\partial p'}{\partial y}. \quad (5)$$

Considering the fluctuations as though they are riding on the mean flow U, Eq. (5) is exactly the same equation as a forced (by the right-hand-side forcing) spring oscillation. The solution of the associated homogeneous equation for v' exhibits a natural oscillation frequency $\omega_{BV\Omega}$,

$$\omega_{BV\Omega}^2 = 2\Omega\left(2\Omega - \frac{\partial U}{\partial y}\right) = f(f + \zeta) = f\zeta_a, \quad (6)$$

where $f = 2\Omega$ is the Coriolis parameter, $\zeta = -\partial U/\partial y$ is relative vorticity, and ζ_a is absolute vorticity. When ζ_a is negative, that is, $\zeta < -f$ in the Northern Hemisphere, the solution for v' may grow exponentially in time. Such a condition is necessary for shear instability. Since the derivation process and the form of equation are similar to the vertical oscillation of a parcel in a stratified fluid, with the oscillation frequency defined by the Brunt–Väisälä frequency (Phillips 1966), the frequency defined in Eq. (6) was called an equivalent Brunt–Väisälä frequency in rotating (nonbuoyant) flows by Bradshaw (1969).

For the jet flow investigated in the present study, the right and left sides of the jet have different stability conditions due to different ''Coriolis force stratification.'' The division between these two sides is marked by zero absolute vorticity ζ_a. On the right side ($\zeta_a < 0$), the flow is destabilized by the negative Coriolis force stratification. On the left side ($\zeta_a > 0$), the flow is stabilized, and the principal angle turns rightward, as shown in Fig. 3. The Reynolds shear stress is suppressed first on the far left side, and then reverses its sign before reaching the division line (recall that the Reynolds shear stress is always negative on the left side of nonrotating jets). These changes correspond respectively to the suppression of turbulence production and the enhancement of mean flow by turbulence eddies, as discussed previously. The sign reversal of the Reynolds shear stress, caused by the Coriolis effects, and the subsequent upgradient momentum transport and eddy-to-mean energy conversion, constitute the key points of this paper.

The effect of the Coriolis force stratification is further illustrated through an analysis of energy redistribution in the simplified horizontal Reynolds stress equations in a two-dimensional flow:

$$\frac{D\overline{u'^2/2}}{Dt} = \overline{u'v'}\zeta + 2\Omega\overline{u'v'} + [\text{OT}], \quad (7a)$$

$$\frac{D\overline{v'^2/2}}{Dt} = -2\Omega\overline{u'v'} + [\text{OT}], \quad (7b)$$

$$\frac{D\overline{u'v'}}{Dt} = \overline{v'^2}\zeta - 2\Omega(\overline{u'^2} - \overline{v'^2}) + [\text{OT}], \quad (7c)$$

where only shear production terms and the Coriolis redistribution terms are kept on the right-hand side for illustration purposes (Tritton 1992). All other terms are lumped into [OT].

When the reference frame (within the rotation system) is rotated by a principal angle β, the Reynolds shear stress vanishes. The equations for the normal stresses (7a,b) then become

$$\frac{D\overline{u_\beta'^2}/2}{Dt} = \frac{1}{2}\overline{u_\beta'^2}\zeta \sin 2\beta + [\text{OT}], \quad (8a)$$

$$\frac{D\overline{v_\beta'^2}/2}{Dt} = -\frac{1}{2}\overline{v_\beta'^2}\zeta \sin 2\beta + [\text{OT}]. \quad (8b)$$

A striking phenomenon stems from the above equation set. In general, the Reynolds normal stresses are first generated by the velocity shear in the mean flow direction and then passed on to the other two directions by pressure–strain correlation (Tennekes and Lumley 1972; Hinze 1975). The normal stress in the mean direction is thus the greatest, which is also evidenced by the fact that $|\beta| < 45°$, as shown in Fig. 3. The rotation effect on turbulence changes the eddy orientation, shifting the principal major axis rightward across the stream. This results in two scenarios. On the far left cyclonic side, where the axis shifts from leaning against the shear to aligning closer to the shear, the Coriolis effects reduce the isotropic tendency of turbulence. When the axis flips over to the other side of the mean flow direction and starts leaning with the shear (Fig. 5), the Coriolis effects take over the process. In other words, the major component of the turbulent energy in the mean direction no longer receives the supply from the mean shear, but becomes diminished instead by powering the mean flow. On the right, anticyclonic side, the Coriolis effects work

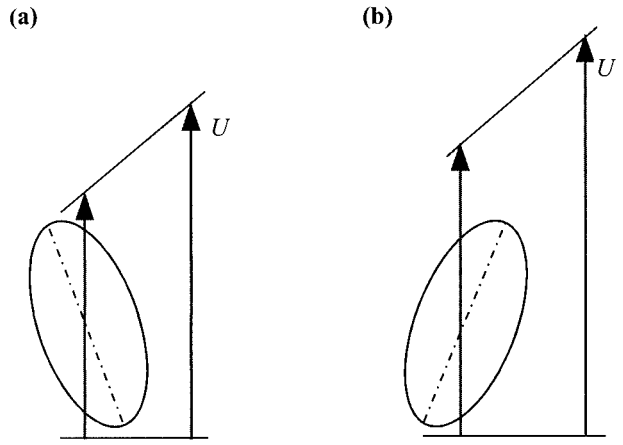

FIG. 5. Schematic of eddy–mean interaction. (a) General case of destabilizing eddy leaning against the mean shear, extracting energy to decelerate the mean flow; (b) cyclonic shear case of stabilizing eddy leaning with the mean shear, supplying energy to accelerate the mean flow. The eddy ellipses represent perturbation streamfunctions at a constant value.

against the pressure–strain redistribution, perpetuating the turbulence toward anisotropy.

The Coriolis effects on turbulence anisotropy can be examined through the turbulence generating process. Rotating the reference frame an angle α the dynamics of the Reynolds shear stress, Eq. (7c) may be expressed as

$$\frac{D\overline{u'_\alpha v'_\alpha}}{Dt} = \left(\frac{1}{2}\zeta + 2\Omega\right)(\overline{v'^2_\alpha} - \overline{u'^2_\alpha}) + \frac{1}{2}\zeta(\overline{u'^2_\alpha} + \overline{v'^2_\alpha})\cos 2\alpha + [\mathrm{OT}]. \quad (9)$$

It is further assumed that this angle follows a fluid parcel where the absolute shear stress is at maximum with respect to temporal variation (Tritton 1992). By omitting [OT], Eq. (9) becomes

$$\cos 2\alpha = \frac{\overline{u'^2_\alpha} - \overline{v'^2_\alpha}}{\overline{u'^2_\alpha} + \overline{v'^2_\alpha}}\left(1 + \frac{2}{\mathrm{Ro}_s}\right), \quad (10)$$

where $\mathrm{Ro}_s = \zeta/2\Omega$ is a local Rossby number, which may take negative values. The path of the maximum shear stress is regarded as the turbulence generating process, and it is shown that its orientation governs and is in the proximity of the orientation of the major principal axis of the Reynolds stress tensor, that is, $\beta \cong \alpha$ (Tritton 1992). Then, Eq. (10) can be expressed in a compact form relating the principal angle, the turbulence ellipticity, and the Rossby number,

$$\cos 2\beta \cong K(1 + 2/\mathrm{Ro}_s). \quad (11)$$

This relationship demonstrates the Coriolis effects on the structure of shear turbulence. When a shear flow is subject to background rotation, the principal angle shifts anticyclonically. In the cyclonic shear side, if K is kept constant, as the background rotation is intensified, Ro_s decreases in positive value and β must decrease in positive value. In the anticyclonic side, as Ro_s increases in negative value, β must still decrease in negative value. In both cases, β shifts anticyclonically, consistent with the experimental results. The experimental results also show that, as rotation intensifies, turbulence eddies are elongated and K increases, which is consistent with the analysis from Eq. (8a,b) above. These structure changes, especially the orientation shift, have a direct effect on eddy–mean flow interaction.

It should be noted that the local Rossby number defined above is different from the global Rossby number used in Fig. 4. Although the local Rossby number was not measured directly, it is reasonable to argue that the bulk value of the local Rossby number is of the same order as the global Rossby number since the turning radius was about the same as the jet width in the present experiment. From the above discussion, it appears that the local Rossby number is a more direct indicator of the Coriolis effects on turbulence generated by strong shear. The strong shear is also present in the cyclonic side of the Gulf Stream, where the local Rossby number is as high as 2 (-2.0 in Fig. 4 of Brooks and Niiler 1977). It was in this region that eddy-to-mean energy conversion was found.

The eddy-to-mean energy conversion has been conceptualized by instability analysis of a two-dimensional flow (e.g., Pedlosky 1987; Bane et al. 1981; Brooks and Bane 1983; Dewar and Bane 1985). Barotropic instability in a two-dimensional flow may be expressed by shear production of turbulent energy,

$$-\overline{u'v'}\frac{dU}{dy} = \overline{\frac{\partial\phi}{\partial x}\frac{\partial\phi}{\partial y}}\frac{dU}{dy} = -\overline{\left(\frac{\partial y}{\partial x}\right)_{\phi=\mathrm{const}}\left(\frac{\partial\phi}{\partial y}\right)^2}\frac{dU}{dy}, \quad (12)$$

where ϕ is the streamfunction of the velocity perturbation. Since $(\partial\phi/\partial y)^2$ is nonnegative and is symmetric with respect to the principal major axis of the eddy ellipse, the sign of the instability depends on the average slope of the stream function, $\overline{(\partial y/\partial x)_{\phi=\mathrm{const}}}$. This slope is exactly the tangent function of the principal angle β. The eddy-to-mean interaction is shown schematically in Fig. 5.

The stabilizing (Fig. 5a) or destabilizing (Fig. 5b) effect of the eddy on the mean shear flow is well established (e.g., Pedlosky 1987). The question that this paper proposes to answer is how the eddy orientation is shifted from one side to the other so as to suppress instability or even to generate stability.

Comparing Fig. 3 with Fig. 5, it is easy to visualize how background rotation affects the principal angle of the turbulence eddies. Equation (11) shows theoretically the effect of rotation on the principal angle. Coriolis effects change the orientation of turbulent eddies, thus changing the energy conversion process, as shown in Eq. (12). In the cyclonic side, when the principal angle becomes smaller, energy transport from the mean flow

to turbulence is suppressed. When the principal angle changes sign, eddy-to-mean energy conversion occurs and the mean flow is accelerated. This provides one possible explanation to the enigma (Brooks and Niiler 1977) of the eddy-to-mean energy conversion occurring on the coastal cyclonic side of the Gulf Stream.

4. Concluding remarks

In this paper, preliminary arguments are presented as a possible explanation for the unusual upgradient momentum transport and associated eddy-to-mean energy conversion observed in the Gulf Stream. Experimental results and theoretical analysis are used to show that Coriolis effects, which are always present in the field, cause anticyclonic shifts of the principal angle of turbulence eddies. The main results of the theoretical analyses of two-dimensional turbulence are a demonstration of how background rotation causes such shifts [Eq. (11)], the effects of Coriolis force stratification [Eq. (6)], and the subsequent effects on momentum transport and eddy–mean interaction [Eq. (12)]. It is recognized that the field situation in the Gulf Stream is much more complicated, involving additional factors not considered in the idealized experiment here. However, the fundamental physics explored in this study should also be present in the field, especially when the cyclonic shear is strong and turbulence is originated from velocity shear. In addition, the range of Rossby numbers considered in the experiments at least partly overlaps observed field values (Brooks and Niiler 1977), though further experiments conducted for smaller Rossby numbers may be helpful to establish a fuller dataset to support the arguments presented here.

It may be of interest to transform Eq. (6) into an equation in terms of local Rossby number,

$$B = \frac{1}{\mathrm{Ro}_s}\left(1 + \frac{1}{\mathrm{Ro}_s}\right), \tag{13}$$

where B is the Bradshaw–Richardson number mentioned in the introduction. This number plays a role for rotating shear flows similar to that of the Richardson number for stratified flows, thus suggesting the term Coriolis force stratification. In other words, when B is negative (positive), the Coriolis effect is destabilizing (stabilizing).

The implication of the Coriolis effect on the principal angle may be profound. As was shown in Dewar and Bane's (1985) study, the direction of mass transport follows the direction of momentum transport. Therefore, compared to a plane jet in a nonrotating background, the Coriolis effects on turbulence may render the jet stream more ''permeable'' for fluxes directed from the coastal ocean to the deep sea. This suggestion, however, requires further study before more definite conclusions can be made.

Acknowledgments. This research was supported by New York Sea Grant Institute under Grant R/CCP-3 and National Science Foundation under Grant OCE 9530197. Two anonymous reviewers are thanked for their comments, which helped to clarify the key points in this paper.

REFERENCES

Bane, J. M., Jr., D. A. Brooks, and K. R. Lorenson, 1981: Synoptic observations of the three-dimensional structure, propagation and evolution of Gulf Stream meanders along the Carolina continental margin. *J. Geophys. Res.,* **86,** 6411–6425.

Bardina, J., J. H. Ferziger, and R. S. Rogallo, 1985: Effect of rotation on isotropic turbulence: Computation and modelling. *J. Fluid Mech.,* **154,** 321–336.

Bidokhti, A. A., and D. J. Tritton, 1992: The structure of a turbulent free shear layer in a rotation fluid. *J. Fluid Mech.,* **241,** 469–502.

Bradshaw, P., 1969: The analogy between streamline curvature and buoyancy in turbulent shear flow. *J. Fluid Mech.,* **36,** 177–191.

Brooks, D. A., and I. M. Bane, Jr., 1983: Gulf Stream meanders off North Carolina during winter and summer 1979. *J. Geophys. Res.,* **88,** 4633–4650.

Brooks, I. H., and P. P. Niiler, 1977: Energetics of the Florida Current. *J. Mar. Res.,* **35,** 163–191.

Cambon, C., and L. Jacquin, 1989: Spectral approach to non-isotropic turbulence subjected to rotation. *J. Fluid Mech.,* **202,** 295–317.

——, J.-P. Benoit, L. Shao, and L. Jacquin, 1994: Stability analysis and large-eddy simulation of rotating turbulence with organized eddies. *J. Fluid Mech.,* **278,** 175–200.

——, N. N. Mansour, and F. S. Godeferd, 1997: Energy transfer in rotating turbulence. *J. Fluid Mech.,* **337,** 303–332.

Dewar, K. W., and J. M. Bane, Jr., 1985: Subsurface energetics of the Gulf Stream near the Charleston Bump. *J. Phys. Oceanogr.,* **15,** 1771–1789.

Godeferd, F. S., 1995: Distorted turbulence submitted to frame rotation: RDT and LES (should be DNS) results. Annual Research Briefs 1995, 175–193. [Available from Center for Turbulence Research, Stanford University, CA 94305.]

Gutmark, E., and I. Wygnanski, 1976: The planar turbulent jet. *J. Fluid Mech.,* **73,** 465–595.

Hinze, J. O., 1975: *Turbulence.* 2d ed. McGraw-Hill, 790 pp.

Ibbetson, A., and D. J. Tritton, 1975: Experiments on turbulence in rotating fluid. *J. Fluid Mech.,* **68,** 639–672.

Jacquin, J., O. Leuchter, C. Cambon, and J. Mathieu, 1990: Homogeneous turbulence in the presence of rotation. *J. Fluid Mech.,* **220,** 1–52.

Johnston, J. P., R. M. Halleen, and D. K. Lezius, 1972: Effects of spanwise rotation on the structure of two-dimensional fully developed turbulent channel flow. *J. Fluid Mech.,* **56,** 533–557.

Kristofferson, R., and H. I. Anderson, 1993: Direct simulation of low-Reynolds-number turbulent flow in a rotating channel. *J. Fluid Mech.,* **256,** 163–197.

Lee, T. N., L. P. Atkinson, and R. Legeckis, 1981: Observations of a Gulf Stream frontal eddy on the Georgia continental shelf, April 1977. *Deep-Sea Res. A,* **28,** 347–378.

Lezius, D. K., and J. P. Johnston, 1971: *The Structure and Stability of Turbulent Wall Layers in Rotating Channel Flow.* Rep. MD, 29, 249 pp. [Available from Thermosciences Division, Dept. of Mechanical Engineering, Stanford University, CA, 94305.]

Lin, G., 1998: Effects of rotation on turbulence in free surface jets. Ph.D. dissertation, State University of New York at Buffalo, 168 pp.

Mansour, N. N., C. Cambon, and C. G. Speziale, 1992: Theoretical and computational study of rotating isotropic turbulence. *Studies in Turbulence,* T. B. Gatski, S. Sarkar, and C. G. Speziale, Eds., Springer-Verlag, 59–75.

Pal, B. K., R. Murthy, and R. Thomson, 1998: Lagrangian measurements in Lake Ontario. *J. Great Lakes Res.,* **24,** 681–697.

Pedlosky, J., 1987: *Geophysical Fluid Dynamics.* 2d ed. Springer-Verlag, 710 pp.

Phillips, O. M., 1966: *The Dynamics of the Upper Ocean.* Cambridge University Press, 261 pp.

Savage, S. B., and R. J. Sobey, 1975: Horizontal momentum jets in rotating basins. *J. Fluid Mech.,* **71,** 755–768.

Schmitz, W. J., Jr., and P. P. Niiler, 1969: A note on the kinetic energy exchange between fluctuation and mean flow in the surface layer of the Florida Current. *Tellus,* **21,** 814–819.

Stommel, H., 1965: *The Gulf Stream: A Physical and Dynamical Description.* 2d ed. University of California Press, 248 pp.

Tennekes, H., and J. L. Lumley, 1972: *A First Course in Turbulence*. The MIT Press, 300 pp.

Tritton, D. J., 1992: Stabilization and destabilization of turbulent shear flow in a rotating fluid. *J. Fluid Mech.,* **241,** 503–523.

Webster, Ferris, 1961a: The effect of meanders on the kinetic energy balance of the Gulf Stream. *Tellus,* **13,** 392–401.

——, 1961b: A description of Gulf Stream meanders off Onslow Bay. *Deep-Sea Res.,* **8,** 130–143.

——, 1965: Measurements of eddy fluxes of momentum in the surface layer of the Gulf Stream. *Tellus,* **17,** 239–245.